J. Virol. doi:10.1128/JVI.01413-18 This is a work of the U.S. Government and is not subject to copyright protection in the United States. Foreign copyrights may apply.

- Plasticity of amino acid residue 145 near the receptor binding site of H3 swine
- influenza A viruses and its impact on receptor binding and antibody 2
- 3 recognition.

JVI Accepted Manuscript Posted Online 24 October 2018

- Short Title: Significance of aa 145 in the HA of H3N2 swine influenza A virus 4
- Jefferson J. S. Santos^a, Eugenio J. Abente^b, Adebimpe O. Obadan^a, Andrew J. Thompson^c, Lucas 5
- Ferreri^a, Ginger Geiger^a, Ana S. Gonzalez-Reiche^{a,d}, Nicola S. Lewis^e, David F. Burke^f, Daniela 6
- S. Rajão^a, James C. Paulson^c, Amy L. Vincent^b and Daniel R. Perez^{a,*}. 7
- 8 a. Department of Population Health, Poultry Diagnostic and Research Center, University of
- 9 Georgia, Athens, Georgia, USA.
- 10 b. Virus and Prion Research Unit, National Animal Disease Center, Agricultural Research
- 11 Service, United States Department of Agriculture, Ames, Iowa, USA
- c. Department of Molecular Medicine, and Immunology & Microbiology, The Scripps 12
- 13 Research Institute, La Jolla, California, USA
- 14 d. Department of Genetics and Genomic Sciences, Icahn School of Medicine at Mount
- 15 Sinai, New York, New York, USA
- e. Department of Pathobiology and Population Sciences 16
- 17 Royal Veterinary College, Hertfordshire, UK
- 18 f. Department of Zoology, University of Cambridge, Cambridge, UK
- 19 *Corresponding author: Department of Population Health, Poultry Diagnostic and Research
- Center, University of Georgia. 953 College Station Road, Athens, GA 30602. 20

- 21 E-mail: dperez1@uga.edu. Phone: 706-542-5506
- Word count: Abstract, 250; Importance, 149; Main text, 5813. 22

Abstract

23

24

25

26

27

28

29

30

31

32

33

34

35

36

37

38

39

40

41

42

The hemagglutinin (HA), a glycoprotein on the surface of influenza A virus (IAV), initiates the virus life cycle by binding to terminal sialic acid (SA) residues on host cells. The HA gradually accumulates amino acid (aa) substitutions that allow IAV to escape immunity through a mechanism known as antigenic drift. We recently confirmed that a small set of aa residues are largely responsible for driving antigenic drift in swine-origin H3 IAV. All identified residues are located adjacent to the HA receptor binding site (RBS), suggesting that substitutions associated with antigenic drift may also influence receptor binding. Among those substitutions, residue 145 was shown to be a major determinant of antigenic evolution. To determine whether there are functional constraints to substitutions near the RBS and their impact on receptor binding and antigenic properties, we carried out site-directed mutagenesis experiments at the single aa level. We generated a panel of viruses carrying substitutions at residue 145 representing all 20 amino acids. Despite limited amino acid usage in nature, most substitutions at residue 145 were well tolerated without major impact on virus replication in vitro. All substitutions retained receptor binding specificity, but frequently led to decreased receptor binding. Glycan microarray analysis showed that substitutions at residue 145 modulate binding to a broad range of glycans. Furthermore, antigenic characterization identified specific substitutions at residue 145 that altered antibody recognition. This work provides a better understanding of the functional effects of aa substitutions near the RBS and the interplay between receptor binding and antigenic drift.

Downloaded from http://jvi.asm.org/ on January 30, 2019 by guest

Importance

44

45

46

47

48

49

50

51

52

53

54

55

56

57

58

59

60

61

62

63

64

65

The complex and continuous antigenic evolution of IAVs remains a major hurdle for vaccine selection and effective vaccination. On the virus' hemagglutinin (HA) of the H3N2 IAVs, the aa substitution N145K causes significant antigenic changes. We show that aa 145 displays remarkable amino acid plasticity in vitro tolerating multiple aa substitutions, many of which have not yet been observed in nature. Mutant viruses carrying substitutions at residue 145 showed no major impairment on virus replication in the presence of lower receptor binding avidity. However, their antigenic characterization confirmed the impact of the 145K substitution in antibody immunodominance. We provide a better understanding of the functional effects of aa substitutions implicated in antigenic drift and its consequences on receptor binding and antigenicity. The mutation analyses presented in this report represent a significant dataset to aid and test computational approaches' ability to predict binding of glycans and in antigenic cartography analyses.

Introduction

The surface hemagglutinin (HA) glycoprotein of influenza A virus (IAV) has a pivotal role in initiating the virus life cycle by binding to the virus receptor on target cells. HA binds to sialic acid (SA) residues that occur as terminal monosaccharides in glycoproteins and glycolipids on the cell surface. SA receptors engaged by IAV are linked to galactose (Gal) in an α 2-3 (SA α 2-3Gal) or α 2-6 (SA α 2-6Gal) linkage configuration (1). Located in a small depression on the globular head of HA, the receptor-binding site (RBS) is composed of the 130-loop, the 150-loop, the 190-helix and the 220-loop. A series of conserved residues, including Tyr98, Ser136, Trp153, and His183 (H3 numbering), forms the base of the RBS and are important for SA interaction (2, 3). Although some HA residues on the RBS are critical for receptor specificity (4-6), other residues may influence binding by modulating virus-receptor binding avidity (7, 8).

67

68

69

70

71

72

73

74

75

76

77

78

79

80

81

82

83

84

85

86

87

88

IAV remains an important pathogen for humans and swine (9). While influenza vaccines are commercially available, the relative effectiveness of these vaccines are heavily dependent on the antigenic match of vaccine strains to circulating virus strains (10, 11). Most of the humoral immune response elicited by influenza vaccination or natural exposure is directed against HA to block virus infection (12, 13). Through a mechanism known as antigenic drift, IAV can circumvent the preexisting antibody response by generating genetic variants during replication with amino acid (aa) substitutions in key HA epitopes on the globular head, allowing for the emergence of escape mutant viruses (14). Antigenic drift is a frequent cause of reduced vaccine effectiveness, especially for H3N2 IAVs (15). Defining the molecular basis of antigenic drift has important implications for understanding IAV evolution and has been facilitated by methodological advances, such as antigenic cartography (16). A recent study identified seven residues (145, 155, 156, 158, 159, 189 and 193) on the globular head of the HA as the major determinants of antigenic drift during the evolution of human H3N2 IAVs (17). Interestingly, all seven residues were located adjacent to the RBS (17), and therefore these residues may also influence receptor binding. The importance of this small set of HA residues as major drivers of antigenic evolution has been demonstrated for IAVs circulating in other hosts, including swine H3N2 IAVs (18). Antigenic changes in human H3N2 IAVs over the course of time were shown to be

frequently caused by a single aa substitution in one of the seven residues, with specific substitutions involved in antigenic change more than once (17). One of those substitutions, N145K, was shown in two separate instances to be the major determinant of antigenic drift during the evolution of human H3N2 IAVs (16, 17). While there is evidence that N145K caused large antigenic changes (7, 16-18) and also altered receptor binding avidity (7), it remains

90

91

92

93

94

95

96

97

98

99

100

101

102

103

104

105

106

107

108

109

110

111

Downloaded from http://jvi.asm.org/ on January 30, 2019 by guest

unclear whether there are functional constraints to substitutions at residue 145 or how alternative aa substitutions at this residue may affect receptor binding and antigenic properties.

In the present study, we carried out site-directed mutagenesis to prepare a panel of H3 HA mutant viruses carrying a single as substitution at residue 145 and subsequently evaluated the impact of substitutions at this key HA residue on receptor binding and antibody recognition. Our data indicates that residue 145 displayed remarkable amino acid plasticity in vitro tolerating multiple aa substitutions, many of which have not yet been observed in nature. Mutant viruses carrying substitutions at residue 145 showed no major impairment on virus replication. While all substitutions retained binding to SAα2-6Gal glycans compared to wild type, mutant viruses with substitutions not commonly found in nature displayed diminished receptor binding capacity. Antigenic characterization confirmed the impact of HA residue 145K in antibody immunodominance. These findings have important implications for understanding virus evolution and aiding the development of novel vaccine design approaches.

Results

HA residue 145 displayed remarkable aa plasticity in vitro. The HA N145K substitution results in significant antigenic changes in both human and swine H3N2 IAVs (7, 16-18). Asparagine (Asn or N) was the most prevalent as found at residue 145 across all analyzed hosts (Fig. 1A). In swine-origin IAVs, around 64% of isolates possessed Asn at residue 145, followed by lysine (Lys or K) at ~33% and serine (Ser or S) at ~2.5%. In human-origin IAVs, about 42% of isolates carried Asn, followed by Ser at ~39% and Lys at ~18%. In avian-origin IAVs, the frequency was ~49% for Asn, ~45% for Ser and ~4.6% for glycine (Gly or G). In canine-origin IAVs, around ~73% of isolates possessed Asn, followed by aspartic acid (Asp or D) at ~24%. In equine-origin IAVs, 99% of isolates carried Asn. Isolates possessing arginine (Arg or R), histidine (His or H),

113

114

115

116

117

118

119

120

121

122

123

124

125

126

127

128

129

130

131

132

133

isoleucine (Ile or I), cysteine (Cys or C), methionine (Met or M), glutamine (Gln or Q), or threonine (Thr or T) at residue 145 were found at a frequency below 1%. Alanine (Ala or A), glutamic acid (Glu or E), leucine (Leu or L), phenylalanine (Phe or F), proline (Pro or P), tryptophan (Trp or W), tyrosine (Tyr or Y) and valine (Val or V) were not observed in any of the isolates from analyzed hosts.

To evaluate the impact of substitutions at residue 145, a panel of viruses carrying single substitutions representing each of the 20 amino acids was generated by reverse genetics (19, 20) (Fig. 1B). Since these viruses were generated in the context of a swine-origin H3N2 IAV (Fig. 1A), 145N, 145K and 145S are referred as naturally occurring substitutions whereas the remaining substitutions are termed alternative or non-naturally occurring. Substitutions were introduced into the HA of A/turkey/Ohio/313053/2004 (H3N2) – herein referred to as OH/04 wt virus that naturally carries 145N (Fig. 1C). Of the 19 OH/04 HA 145 single aa mutant viruses rescued, next generation sequencing analysis revealed that 12 substitutions (145A, 145C, 145G, 145H, 145K, 145L, 145M, 145P, 145Q, 145R, 145S and 145T) were well tolerated (98-100% of sequenced reads possessed the expected codon at residue 145) after 3 passages in MDCK cells. For substitutions 145F, 145I, 145V and 145Y, the percentage of reads bearing the mutated codon was around 90% while the remaining 10% of reads showed a partial reversion to the wt codon (I145N, V145N and Y145N) or a partial transition for a codon specifying Ser (F145S). None of these HA substitutions led to compensatory substitutions on the HA or neuraminidase (NA) segments. Three substitutions (145D, 145E and 145W) were not well tolerated, leading to partial reversion to the wt codon (D145N) or partial transition to a codon specifying either Gly (E145G) or Leu (W145L). Moreover, additional substitutions emerged on the HA for 145E and 145W

Downloaded from http://jvi.asm.org/ on January 30, 2019 by guest

135

136

137

138

139

140

141

142

143

144

145

146

147

148

149

150

151

152

153

154

155

156

(T128A) or on the NA for 145E (T148I). For these reasons 145D, 145E and 145W viruses were excluded from further analysis.

Viruses were assayed for their ability to agglutinate red blood cells (RBCs) from different species (turkey, chicken, and horse) by standard hemagglutination (HA) assay. Turkey and chicken RBCs are known to carry both SAα2-3Gal and SAα2-6Gal receptors on their cell surface while horse RBCs mainly display SAα2-3Gal (21-23). Similar to 145N (wt) virus, nearly all mutant viruses were found to agglutinate turkey RBCs efficiently, with the exception of 145C virus that displayed low HA titers (Table 2). In contrast, agglutination of chicken RBCs was less consistent with HA titers of some mutant viruses comparable to that of the 145N (wt) virus while other mutant viruses exhibited an 8 to 16-fold decrease in HA titers (145F, 145G, 145V and 145Y viruses) or no agglutination (145C virus) (**Table 2**). Only the 145F virus showed detectable, albeit low, HA titers using horse RBCs (Table 2). There was no correlation between the ability to agglutinate RBCs and virus titers. Due the decreased ability to agglutinate RBCs, the 145C virus was not tested in further assays.

Viruses were then compared in a multiple-step infection cycle in vitro. MDCK cells were infected at a low multiplicity of infection (MOI of 0.01). All viruses grew to high titers and displayed similar growth kinetics (Fig. 2A). There was no discernable difference in peak titers (~6.5 to 7.0 log₁₀ TCID₅₀/ml equivalents) at 72 hpi, with the exception of 145P and 145H viruses that showed slightly lower peak titers ($\sim 5.5 \log_{10} \text{TCID}_{50}/\text{ml}$ equivalents, P < 0.001). Taken together, these results indicate that residue 145 shows high levels of plasticity in vitro despite of the limited detection of a variation in nature. Furthermore, single as substitutions did not have a major impact in growth kinetics in vitro but modulated the ability of mutant viruses to agglutinate RBCs from particular hosts.

158

159

160

161

162

163

164

165

166

167

168

169

170

171

172

173

174

175

176

177

178

179

Viruses with alternative substitutions at residue 145 retain SAα2-6Gal binding, but frequently displayed decreased receptor binding avidity. To further expand on the receptor binding characterization of the 145 mutants, we analyzed whether these substitutions were involved in modulating receptor avidity or receptor specificity by measuring agglutination of turkey RBCs previously treated with different concentrations of bacterial neuraminidase (Fig. 2B-C). All of the mutant viruses bound to desialylated RBCs to a varying degree. Naturally occurring substitutions showed the highest avidity to receptors. Binding of 145N (wt) virus was indistinguishable from either the 145K (both neuraminidases) or 145S (C. perfringens neuraminidase) viruses. Nearly all mutant viruses carrying alternative substitutions at residue 145 displayed decreased receptor binding avidity, with the notable exception of 145M virus that showed no discernable difference in binding compared to 145N (wt) virus. Overall, the results suggest differences in avidity regardless of the bacterial neuraminidases tested, although specificity cannot be completely ruled out. Next, we performed a glycan-based ELISA using monospecific preparations of Fet-HRP as surrogates of binding to SAα2-3Gal (3-Fet-HRP) or SAα2-6Gal (6-Fet-HRP) (24) glycans

(Fig. 3A-P). The assay reliably discriminated receptor binding specificity as evidenced by the viruses used as controls, with human pH1N1 showing a preference to SAα2-6Gal (Fig. 3Q) while avian Δ H5N1 displayed restricted binding to SA α 2-3Gal (**Fig. 3R**). All of the mutant viruses retained binding to $SA\alpha 2$ -6Gal with no residual binding to $SA\alpha 2$ -3Gal. Naturally occurring substitutions [145N (wt), 145K and 145S viruses] showed the greatest binding to SAα2-6Gal (Fig. 3A, G and M). Consistent with differences in avidity from previous results, mutant viruses carrying alternative substitutions at residue 145 displayed weaker binding to SAα2-6Gal (Fig. 3B-F, H-L and N-P) compared to viruses possessing naturally occurring

181

182

183

184

185

186

187

188

189

190

191

192

193

194

195

196

197

198

199

200

201

202 with the glycan-based ELISA results, these data indicated that while certain substitutions in HA 9

substitutions. Among mutant viruses carrying alternative substitutions, 145M and 145P viruses demonstrated the highest binding (Fig. 3I and J) while 145F and 145G showed substantial decrease in binding to $SA\alpha 2$ -6Gal (**Fig. 3C and D**). Overall, these results suggest substitutions in HA at residue 145 do not affect receptor specificity but modulate receptor avidity. Nearly all the alternative substitutions led to decreased receptor binding avidity. Substitutions at residue 145 modulate binding to a broad range of $SA\alpha 2$ -6Gal glycans. To further compare the impact of substitutions at residue 145 on receptor binding specificity, glycan array analysis was performed for all viruses using a glycan microarray containing linear, Olinked, and N-linked glycans with extended poly-N-acetyl-lactosamine (poly-LacNAc) repeats found in human, swine and ferret airway tissues (25). The array provides a broad semiquantitative view of the binding preference for specific viruses. All of the viruses retained specificity to $SA\alpha 2$ -6Gal glycans (**Fig. 4A-P**), corroborating the results from the glycan-based ELISA (Fig. 3). Viruses carrying naturally occurring substitutions showed expanded binding to nearly all SAα2-6Gal glycan types in the array. OH/04 wt (145N) virus had slightly preferred binding to O-glycans (**Fig. 4A**) while 145K virus appeared to favor binding to N-glycans (**Fig. 4G**). 145S virus binding showed a slight reduction in binding to linear and some of the smaller O-glycans (Fig. 4M) compared to OH/04 wt (145N) virus (Fig. 4A). There were distinct patterns of binding for viruses carrying alternative substitutions. 145F, 145L, 145M, 145P 145Q, 145T and 145V viruses demonstrated binding to a broader range of glycans that was comparable to OH/04 wt (145N) virus (Fig. 4C, H, I-K, N and O). The 145A, 145G, 145H, 145I, 145R and 145Y mutant viruses displayed a more restricted binding to glycans in the array, although they appear to maintain a preference to O-linked glycans (Fig. 4B, D, E, F, L and P). Taken together

Downloaded from http://jvi.asm.org/ on January 30, 2019 by guest

204

205

206

207

208

209

210

211

212

213

214

215

216

217

218

219

220

221

222

223

224

225

at residue 145 lead to broad reductions in binding to SAα2-6Gal glycans, many non-natural variants appear to be well-tolerated, with only minor variance in receptor specificity detected. Substitutions at residue 145 modulate sera reactivity. For human H3N2 IAVs, it has been proposed that the emergence of the HA N145K substitution led to a change in antibody immunodominance (7). To assess whether a similar phenomenon occurs in swine-origin H3 IAVs and how alternative substitutions at residue 145 affect antigenicity, the sera reactivity of each mutant virus in the panel was tested by ELISA (Fig. 5A-C) and HI assays (Fig. 6A and B). For these experiments, swine antisera against NY/11 or IA/14 wild type viruses were tested. The HA1 domain of these viruses differs by only two amino acids: NY/11 virus possesses 145N/289P while IA/14 carries 145K/289S. Based on its location at the base of the HA1 globular head and no prior evidence of an antigenic role, we assume that position 289 is antigenically irrelevant. Additionally, swine antisera against OH/04 wt virus were tested. To prevent confounding effects, the HA gene segment of the NY/11 and IA/14 viruses were rescued by reverse genetics in the background of 7 gene segments from the OH/04 wt virus. The 1+7 NY/11 and IA/14 reverse genetics viruses were used as controls in ELISA and HI assays. Reactivity of sera generated against the OH/04 wt virus was similar across the entire panel of OH/04 145 single as mutant viruses (Fig. 5A), indicating substitutions at residue 145 in the context of OH/04 HA do not change antigenicity against wt homologous sera. Consistent with amino acid divergence between OH/04 wt and control viruses, OH/04 wt virus antisera had reduced reactivity to both NY/11 and IA/14 control viruses. Surprisingly, sera raised against the NY/11 virus displayed no discernible difference in reactivity among all of the virus evaluated regardless of the 145 as substitution, including the NY/11 and IA/14 viruses (Fig. 5B). As

Downloaded from http://jvi.asm.org/ on January 30, 2019 by gues

observed for human H3N2 IAVs, the presence of 145K in a swine-origin IAV results in an

227

228

229

230

231

232

233

234

235

236

237

238

239

240

241

242

243

244

245

246

247

248

immunodominant epitope targeted by the antibody response (Fig. 5C). Sera generated against the IA/14 virus showed decreased reactivity to the NY/11 virus (possessing HA residue 145N) compared to the IA/14 virus (carrying HA residue 145K). Nearly all of the OH/04 145 single aa mutant viruses, with the exception of 145K virus, exhibited diminished reactivity to the IA/14 virus antisera. The 145K virus was the only mutant virus to consistently show reactivity more similar to homologous IA/14 sera generated against the IA/14 virus, confirming the impact of HA residue 145K in modulating antibody immunodominance.

Antigenic characterization by HI assay was mostly consistent with the ELISA data. The OH/04 wt virus antisera reacted to all OH/04 145 single aa mutant viruses. Relative to the 145N (wt) virus, changes in HI titers were almost indistinguishable (Fig. 6A and B). The OH/04 wt virus antisera had a large reduction in cross-HI reactivity against the IA/14 virus and only a modest reduction against the NY/11 virus. Similar to the ELISA data, most substitutions at residue 145 minimally affected NY/11 virus antisera reactivity, with the 145K virus causing the largest reduction in cross-HI titers. Reactivity of the IA/14 virus antisera was drastically reduced against nearly all of the OH/04 145 single as mutant viruses. In agreement with previous results, the 145K virus was the only mutant virus to show minimal reduction in sera cross-reactivity compared to IA/14 virus. Collectively, these results indicate that residue 145K has a profound impact in modulating antibody immunodominance and that sera raised against a 145K bearing virus can recognize the epitope bearing such substitution in the context of a distinct H3 HA.

Downloaded from http://jvi.asm.org/ on January 30, 2019 by guest

Discussion

HA engagement with terminal SA residues on host cells is an essential step in the IAV's replication cycle. Not surprisingly, receptor-binding specificity is a major host range restriction factor. In a simplistic view, IAVs of avian origin prefer binding to SAα2-3Gal glycans whereas

250

251

252

253

254

255

256

257

258

259

260

261

262

263

264

265

266

267

268

269

270

271

those that circulate in humans favor binding to SAα2-6Gal receptors (5, 26-28). During human adaptation of avian-origin IAVs, receptor specificity switch is accompanied by specific substitutions on the HA (E190D/G225D in the H1 subtype and Q226L/G228S in the H2 and H3 subtypes) (5, 26, 29, 30). While these residues are critical to receptor binding specificity, other residues on the HA have the potential to affect receptor binding functions, including receptor binding avidity (7, 8, 23, 31). The identification of up to 7 residues (145, 155, 156, 158, 159, 189 and 193) near the RBS as the major determinants of antigenic drift during the evolution of human and swine H3N2 IAVs (17, 18, 32) has led to the hypothesis that emerging substitutions in these residues must drive antigenic change and immune escape without disrupting receptor binding properties, potentially limiting the flexibility of an residues in these positions (17, 33). In agreement with this hypothesis, analysis of HA sequences showed the occurrence of only a small subset of an substitutions at these residues that are recycled sporadically (17, 18, 32, 34, 35). Here we examined the amino acid plasticity at residue 145, one of the identified key determinants of antigenic drift, by mutating this residue to create a panel of H3 HA mutant viruses carrying a single aa substitution representing every possible amino acid in a swine H3N2 backbone. HA residue 145 showed extraordinary plasticity with 16 out of 19 substitutions (145A, 145C, 145F, 145G, 145H, 145I, 145K, 145L, 145M, 145P, 145Q, 145R, 145S, 145T, 145V and 145Y) being well tolerated in vitro (90-100% of sequenced reads possessing the mutated codon at residue 145). Whether these substitutions are tolerated in vivo is beyond the scope of the present report and remain to be determined. Consistent with the intricate balance between immune escape and receptor binding, three substitutions (145D, 145E and 145W) were not tolerated and led to the emergence of partial reversion at residue 145 and additional

Downloaded from http://jvi.asm.org/ on January 30, 2019 by gues

substitutions in either HA (T128A) and/or NA (T148I). HA T128A disrupted a potential

273

274

275

276

277

278

279

280

281

282

283

284

285

286

287

288

289

290

291

292

293

294

glycosylation site (36, 37) and was shown to emerge along with a substitution at residue 145 in human H3N2 IAVs during the 2013-2014 season (34). NA T148I has been associated with reduced NA activity, decreased susceptibility to neuraminidase inhibitors, and NA-mediated binding and agglutination (38, 39). The previously reported role of these substitutions suggests they may be compensatory.

With the exception of 145C virus, there was no discernible difference in the ability of tested mutant viruses to agglutinate turkey RBCs. Turkey and chicken RBCs carry both SAα2-3Gal and SAα2-6Gal glycans on their cell surface (21-23), and some of tested mutant viruses exhibited impaired ability to agglutinate chicken RBCs. Loss of the ability to agglutinate RBCs has plagued the antigenic characterization of recent human H3N2 IAVs (40). As previously reported for chicken RBCs (41), an in-depth analysis of major glycan structures present on RBCs from other hosts will help shed light to current issues on antigenic characterization of IAVs.

Using independent assays, we demonstrated that all tested mutant viruses retained some binding to SA\alpha2-6Gal glycans. However, viruses possessing naturally occurring substitutions [145N (wt), 145K and 145S] showed the strongest receptor binding. With the exception of 145M virus, all viruses carrying alternative substitutions (145A, 145C, 145F, 145G, 145H, 145I, 145L, 145P, 145Q, 145R, 145T, 145V and 145Y) displayed decreased ability to bind SAa2-6Gal receptors. In contrast to other reports, no compensatory substitutions were identified on the HA or NA by next-generation sequencing (42, 43). This indicates that the observed changes in receptor binding reported here are directly related to substitutions at residue 145. It is important to emphasize that although viruses carrying alternative substitutions exhibited decreased receptor binding avidity in vitro, the lower threshold for biologically relevant avidity in vivo is unknown. Glycan array analysis revealed a broad range of SAα2-6Gal glycan interactions that were

296

297

298

299

300

301

302

303

304

305

306

307

308

309

310

311

312

313

314

315

316

317

modulated by substitutions at residue 145. Interestingly, one of the viruses with the lowest binding to 6-modified fetuin glycans in the panel (145F virus) displayed extensive binding to SAα2-6Gal glycans, including extended glycans (25). While the expanded glycan array provides important insights on the binding preference, which receptors are relevant for IAV attachment and transmission in vivo remain to be elucidated. Furthermore, the density, distribution and organization of glycans on host tissues are poorly defined.

As observed in human H3N2 IAVs, the emergence of the HA N145K substitution in swine H3N2 IAVs led to a change in the antibody immunodominance. It is astonishing that reactivity to sera raised against a virus possessing HA 145N was indistinguishable among all of the viruses carrying substitutions at residue 145, but reactivity to sera raised against a virus possessing HA 145K was highly skewed to recognize an epitope bearing HA residue 145K even in the context of a distantly related H3 HA, demonstrating the dramatic impact N145K mutants can have in population immunity. Antibody immunodominance may be key for understanding antigenic drift and refers to the immunological phenomenon in which the immune system preferentially mounts a response to complex antigens in a dynamic hierarchical order (14). Immunodominance hierarchy can occur at the level of viruses within multivalent immunogens, proteins within viruses, antigenic sites within proteins, epitopes within antigenic sites and, as showed in the present report and by others, single as substitutions within epitopes (7, 14, 16, 17, 44, 45). The impact of substitutions at residue 145 on immunogenicity and antibody immunodominance remains to be fully characterized. While there may be a fitness cost associated with the emergence of such substitutions in nature, the ability to manipulate the aa plasticity near the RBS may offer an alternative approach to induce broader protection and, perhaps, potentially elicit receptor mimicry, broad-spectrum neutralizing antibodies (46).

Downloaded from http://jvi.asm.org/ on January 30, 2019 by gues

319

320

321

322

323

324

325

326

327

328

329

330

331

332

333

334

335

336

337

338

339

340

The complex and continuous antigenic evolution of IAVs remains a major hurdle for vaccine selection and effective vaccination. We provide a better understanding of the functional effects of an substitutions near the RBS implicated in antigenic drift and its consequences on receptor binding. The mutation analyses presented in this report represent a significant dataset to aid and test computational approaches' ability to predict binding of glycans. **Materials and Methods**

Cell culture. Madin-Darby canine kidney (MDCK) and human embryonic kidney 293T cells were maintained in Dulbecco's modified Eagle's medium (DMEM) supplemented with 10% fetal bovine serum (FBS). Cells were propagated at 37°C in a humidified incubator under 5% CO₂ atmosphere. Molecular cloning and virus rescue. The OH/04 wt strain is a prototypic swine-origin virus amenable to genetic manipulation by an established reverse genetics (RG) system (18, 47, 48). Single as substitutions representing each of the 20 naturally occurring amino acids (**Table 1**) were inserted by site-directed mutagenesis at the codon corresponding to HA residue 145 (H3 numbering). To prevent the carryover of OH/04 wt HA plasmid DNA during PCR amplification, the cloned OH/04 wt HA segment was split into two overlapping plasmids: pDP-SD1 and pDP-SD2. The pDP-SD1 plasmid carries the mouse RNA polymerase I terminator (t1) (20) followed by nucleotides 1-522 of OH/04 wt HA segment. The pDP-SD2 plasmid contains nucleotides 500-1762 of OH/04 wt HA segment followed by the human RNA polymerase I promoter (poll) (20). To introduce the desired mutations into OH/04 wt HA, a PCR fragment containing t1 followed by the 5' portion of the HA was generated with forward primer 5'-ACC GGA GTA CTG GTC GAC CTC CGA AGT TGG GGG GGA GCA AAA GCA GG-3' and the respective reverse primer (Table 1) using pDP-SD1 as template. Similarly, a PCR fragment comprising the

342

343

344

345

346

347

348

349

350

351

352

353

354

355

356

357

358

359

360

361

362

363

CTG ACA ACG TCC CCG GCC CGG CGC TGC T-3' and the respective forward primer (Table 1). All PCR products were purified by gel extraction using QIAquick Gel Extraction Kit (Oiagen, Valencia, CA) and combined to produce RG-ready PCR-based HA segments for individual OH/04 HA 145 single as mutants by overlapping PCR as previously described (19). All PCR reactions were performed with Phusion High Fidelity DNA polymerase (New England Biolabs, Ipswich, MA) and confirmed to be free of unwanted mutations by sequencing. Viruses were rescued by PCR-based RG using a co-culture of 293T/MDCK cells as previously described (19, 20). To generate OH/04 HA 145 single as mutant viruses, the respective RG PCR-based HA segment was paired with the seven plasmids representing the remaining OH/04 wt gene segments. Following transfection, cells were incubated at 35°C. After 24 h incubation, media was replaced with Opti-MEM I (Life Technologies, Carlsbad, CA) containing 1 μg/mL TPCKtrypsin (Worthington Biochemicals, Lakewood, NJ) and 1% antibiotics/antimycotic solution (Sigma-Aldrich, St. Louis, MO). Following virus rescue, virus stocks were amplified in MDCK cells. Virus stocks were titrated by tissue culture infectious dose 50 (TCID₅₀) and virus titers were determined by the Reed and Muench method (49). Whole-genome sequencing. Virus RNA from tissue culture supernatant virus stocks were purified using the RNeasy mini kit (Qiagen, Valencia, CA) or MagNA Pure LC RNA Isolation Kit (Roche Life Science, Mannheim, Germany). Isolated virus RNA served as template in a onestep reverse transcriptase PCR (RT-PCR) reaction for multi-segment, whole genome amplification (50). Amplicon sequence libraries were prepared as previously described (50) or using Nextera XT DNA Library Prep Kit (Illumina, San Diego, CA) according to the manufacturer's protocol. Barcoded libraries were multiplexed and sequenced on the high-

3' portion of HA followed by poll was amplified from pDP-SD2 using reverse primer 5'-ATG

365

366

367

368

369

370

371

372

373

374

375

376

377

378

379

380

381

382

383

384

385

386

throughput Illumina MiSeq sequencing platform in a paired-end 150 nt run format. De novo genome assembly was performed as described previously (50) and HA and NA-specific reads were mapped to OH/04 reference sequences using Geneious 10.1.3 (51). In vitro growth kinetics. Confluent monolayers of MDCK cells were inoculated at 0.01 multiplicity of infection (MOI) for each virus. After 1 h incubation, virus inoculum was removed, and cells washed twice with 1X phosphate-buffered saline (PBS). Then, Opti-MEM I (Life Technologies, Carlsbad, CA) containing TPCK-trypsin (Worthington Biochemicals, Lakewood, NJ) and antibiotics/antimycotic solution (Sigma-Aldrich, St. Louis, MO) was added to the cells. At indicated time points, tissue culture supernatant from inoculated cells was collected for virus titer quantification. Virus RNA from tissue culture supernatant was isolated using the MagMAX-96 AI/ND Viral RNA Isolation Kit (Thermo Fisher Scientific, Waltham, MA). Virus titers were determined using a real-time reverse transcriptase PCR (rRT-PCR) assay based on the influenza A matrix gene (52). The rRT-PCR was performed in a LightCycler 480 Real Time PCR instrument (Roche Diagnostics, Rotkreuz, Switzerland) using the LightCycler 480 RNA Master Hydrolysis Probes kit (Roche Life Science, Mannheim, Germany). A standard curve was generated using 10-fold serial dilutions from an OH/04 wt virus stock of known titer to correlate qPCR crossing point (Cp) values with virus titers, as previously described (53). Virus titers were expressed as $\log_{10} \text{TCID}_{50}/\text{ml}$ equivalents. Hemagglutination (HA) assay. Chicken (Poultry Diagnostic and Research Center, Athens, GA), turkey (Poultry Diagnostic and Research Center, Athens, GA) and horse (Lampire Biologicals, Pipersville, PA) red blood cells (RBCs) were prepared from whole blood preparations using standard techniques (54). Virus HA assays were carried out using 0.5% (vol/vol in PBS) chicken RBCs, 0.5% (vol/vol in PBS) turkey RBCs or 1% (vol/vol in PBS) horse RBCs. Briefly, 50 µl of

388

389

390

391

392

393

394

395

396

397

398

399

400

401

402

403

404

405

406

407

408

409

RBC preparations was added to 50 µl of two-fold serial dilutions of virus stocks allowed to incubate at room temperature for 45 min. After incubation agglutination was measured, and data expressed as the inverse of the highest dilution that allowed full agglutination. Receptor cell binding assay. The receptor cell binding assay was performed as previously described (8, 18, 55). Briefly, 10% (vol/vol in PBS) turkey RBCs were pretreated for 1 h at 37°C with two-fold serial dilutions of bacterial neuraminidase from Arthrobacter ureafaciens (New England BioLabs, Ipswich, MA) or Clostridium perfringens (New England BioLabs, Ipswich, MA). Following neuraminidase treatment, treated RBCs were then washed twice with cold PBS, and then resuspended to 1% (vol/vol in PBS). 50 µl of 1% RBCs treated with the different neuraminidase concentrations were added to 50 µl of each virus (8 HAU, as determined on untreated RBCs) and allowed to incubate at room temperature for 45 min. After incubation agglutination was measured, and data expressed as the maximal concentration of neuraminidase that allowed full agglutination. Solid-phase assay of receptor binding specificity. The receptor-binding specificity was determined in a solid phase direct binding assay using monospecific preparations of peroxidase (HRP)-conjugated fetuin (fet-HRP). Monospecific preparations of fet-HRP were synthesized using α2-3-sialyltransferase from *Pasteurella multocida* (Sigma, St. Louis, MO) for 3-modified fetuin (3-fet-HRP) or α2-6-sialyltransferase from *Photobacterium damsela* (Sigma, St. Louis, MO) for 6-modified fetuin (6-fet-HRP), essentially as described previously (24). 96-well native fetuin-coated flat-bottom plates (Greiner Bio-One, Monroe, NC) were incubated overnight at 4°C with 128 HAU of each virus in 0.02 M tris-buffered saline (TBS), pH 7.2-7.4. Virus samples were run in duplicate. Plates were washed three times with PBS and blocked with blocking solution [BS, PBS containing 0.1% neuraminidase-treated bovine serum albumin (BSA-NA)] for

Downloaded from http://jvi.asm.org/ on January 30, 2019 by guest

411

412

413

414

415

416

417

418

419

420

421

422

423

424

425

426

427

428

429

430

431

432

2 h at room temperature. After blocking, plates were washed twice with ice-cold washing solution (WS, PBS containing 0.02% Tween 80) and incubated with two-fold serial dilution of 3-Fet-HRP (SAα2-3Gal) or 6-Fet-HRP (SAα2-6Gal) in reaction solution (RS, PBS containing 0.02% Tween-80, 0.1% BSA-NA and 2 µM oseltamivir carboxylate) for 1 h at 4°C. After incubation, plates were washed five times with ice-cold WS before adding freshly prepared substrate solution (SS, 0.01% 3,3',5,5'-tetramethylbenzidine in 0.05 M sodium acetate with 0.03% H₂O₂). Reactions were allowed to proceed at room temperature for 30 min unless otherwise stated. Reactions were stopped with 3% (vol/vol in ddH₂O) H₂SO₄. Absorbance readings were obtained at 450 nm using a Victor x3 Multilabel Plate Reader (PerkinElmer, Waltham, MA). Glycan array analysis. Virus stocks were grown in MDCK cells, clarified by low-speed centrifugation, and inactivated by treatment with 0.1% β-propiolactone (BPL) for 1 day at 4°C. Inactivated virus stocks were concentrated as described previously (56). Concentrated virus stocks were resuspended in PBS with 5% glycerol to HAU, aliquoted and stored at -80°C. HA titers of concentrated virus stocks were determined by HA assay using 0.5% (vol/vol in PBS) turkey RBCs. Glycan array analysis was performed using an NHS ester-coated glass microarray slide containing six replicates of 128 diverse synthetic sialic acid-containing glycans, including terminal sequences as well as N-linked and O-linked glycans found on mammalian and avian glycoproteins and glycolipids (25). Whole influenza virus samples were diluted to 256 HAU in PBS containing 3% BSA (PBS-BSA) and incubated on the array surface for 1 h at room temperature in a humidity-controlled chamber. After incubation, slides were washed in PBS and incubated with OH/04 wt swine antisera (18) diluted 1:200 in PBS-BSA for 1 h. Slides were

washed in PBS and incubated for 1 h in goat anti-pig IgG conjugated to fluorescein

433 isothiocyanate (FITC; Thermo Fisher Scientific, Waltham, MA) diluted in PBS-BSA (20 µg/ml 434 final concentration). Slides were washed twice in PBS, and in dH₂O, then dried prior to 435 detection. Slide scanning to detect bound virus was conducted using an InnoScan 1100AL 436 (Innopsys, Carbonne, France) fluorescent microarray scanner. Fluorescent signal intensity was 437 measured using Mapix (Innopsys, Carbonne, France) and mean intensity minus mean 438 background of 4 replicate spots was calculated. A complete list of the glycans present in the 439 array is presented in **Supplementary Table 1**. The array is comprised of non-sialoside control 440 (1-10; Grey), SAα2-3Gal (11-76; Yellow) and SAα2-6Gal (77-128; Green) glycans. Glycans are 441 grouped by structure type: L, linear; O, O-linked; N, N-linked and L^x, sialyl Le^x. 442 Antisera. Swine antisera against A/swine/New York/A01104005/2011 (H3N2) [NY/11], 443 A/swine/Iowa/A01480656/2014 (H3N2) [IA/14] and A/turkey/Ohio/313053/2004 (H3N2) 444 [OH/04] were generated in previous studies (18, 32). For each virus, two pigs were primed and 445 boosted intramuscularly with UV-inactivated whole virus vaccine prepared with commercial oil-446 in-water adjuvant (1:5 ratio; Emulsigen D, MVP Laboratories, Inc., Ralston, NE). The pigs were 447 humanely euthanized for blood collection. 448 Hemagglutination inhibition (HI) assay. HI assays were performed as previously described (54). 449 Prior to HI testing, swine antisera were treated overnight with receptor-destroying enzyme 450 (Denka Seiken, Tokyo, Japan) and heat inactivated at 56°C for 30 min. Serial two-fold dilutions 451 starting at 1:10 were tested for the ability to inhibit the agglutination of 0.5% turkey RBCs with 4 452 HAU of each virus. HI titers were recorded as the inverse of the highest dilution that inhibited 453 hemagglutination. 454 Enzyme-linked immunosorbent assay (ELISA). For ELISA, 96-well flat-bottom plates (Greiner Bio-One, Monroe, NC) were incubated overnight at 4°C with 16 HAU of each virus in 1X 455

457

458

459

460

461

462

463

464

465

466

467

468

469

470

471

472

473

474

475

476

477

478

coating solution (Seracare, Milford, MA). Virus samples were run in duplicate. Plates were blocked with StartingBlock (PBS) blocking buffer (Thermo Fisher Scientific, Waltham, MA) for 1 h at room temperature. After blocking, plates were washed three times with PBS containing 0.05% tween 20 (PBS-T). Two-fold serial dilutions of swine antisera were added and allowed to incubate for 1 h at room temperature. After incubation, plates were washed three times with PBS-T before adding the secondary goat anti-swine IgG-HRP HRP-conjugated polyclonal antibody (Seracare, Milford, MA). Plates were incubated at room temperature for 1 h. After incubation, plates were washed three times with PBS-T before adding freshly prepared SS buffer or 2, 2'-azino-di(3-ethylbenzthiazoline-6-sulfonate) [ABTS] 1-component microwell peroxidase substrate (Seracare, Milford, MA) for 1 h at room temperature. The reaction was stopped by adding 3% (vol/vol in ddH₂O) H₂SO₄ or ABTS peroxidase stop solution (Seracare, Milford, MA), respectively. Absorbance readings were obtained at 405 nm using a Victor x3 Multilabel Plate Reader (PerkinElmer, Waltham, MA). Statistical analysis. All statistical analyses were performed using the GraphPad Prism Software Version 7 (GraphPad Software Inc., San Diego, CA). For multiple comparisons, one-way or twoway ANOVA followed by a post-hoc Tukey test were performed. When indicated, a P value below 0.05 (P<0.05) was considered significant. Structure modeling. A model of the structure of the HA of A/turkey/Ohio/313053/2004 (H3N2) was built by homology modeling using Modeller v9.16 (57) based upon the crystal structure of multiple H3 HA proteins [Protein Data Bank (PDB) codes 2YP7, 1HA0, 2YP2, 4WE8 and 4WE5). The generated model was subsequently rendered with PyMOL v2.1 (58). Computational analysis of HA sequences. The frequency distribution of an identities at residue 145 (H3 numbering) was computed using the sequence variation analysis tool in the Influenza

480

481

482

483

484

485

486

487

488

489

490

491

492

493

494

Research Database (IRD) (59). HA aa sequences from IAVs of the H3 subtype isolated from swine, human, avian, canine and equine hosts and publicly available in the IRD as of September 06, 2017 were analyzed. For humans, the frequency was calculated from precomputed data in the IRD database. Only amino acids that reached a frequency of at least 1% are labeled in the plot legend.

Acknowledgements

This study was supported by a subcontract from the Center for Research on Influenza Pathogenesis (CRIP) to DRP under contract HHSN272201400008C from the National Institute of Allergy and Infectious Diseases (NIAID) Centers for Influenza Research and Surveillance (CEIRS) and by NIH grant AI114730 to JCP. JJSS received a short-term training award from the NIAID CEIRS Training Program, HHSN272201400008C. Additional funding was supplied by the Kwang Hua Educational Foundation to JCP. This study was also supported in part by resources and technical expertise from the Georgia Advanced Computing Resource Center, a partnership between the University of Georgia's Office of the Vice President for Research and Office of the Vice President for Information Technology.

References

- 495 1. Nicholls JM, Chan RW, Russell RJ, Air GM, Peiris JS. 2008. Evolving complexities 496 of influenza virus and its receptors. Trends Microbiol 16:149-157.
- 497 2. Wilson IA, Skehel JJ, Wiley DC. 1981. Structure of the haemagglutinin membrane 498 glycoprotein of influenza virus at 3 A resolution. Nature **289:**366-373.
- 499 Skehel JJ, Wiley DC. 2000. Receptor binding and membrane fusion in virus entry: the 500 influenza hemagglutinin. Annu Rev Biochem 69:531-569.

301	4.	Mati osovicii Mi, Tuzikov A, Dovini M, Gainbai yan A, Kinnov A, Casti ucci Mik,
502		Donatelli I, Kawaoka Y. 2000. Early alterations of the receptor-binding properties of
503		H1, H2, and H3 avian influenza virus hemagglutinins after their introduction into
504		mammals. J Virol 74: 8502-8512.
505	5.	Connor RJ, Kawaoka Y, Webster RG, Paulson JC. 1994. Receptor specificity in
506		human, avian, and equine H2 and H3 influenza virus isolates. Virology 205:17-23.
507	6.	Wan H, Perez DR. 2007. Amino acid 226 in the hemagglutinin of H9N2 influenza
508		viruses determines cell tropism and replication in human airway epithelial cells. J Virol
509		81: 5181-5191.
510	7.	Li Y, Bostick DL, Sullivan CB, Myers JL, Griesemer SB, Stgeorge K, Plotkin JB,
511		Hensley SE. 2013. Single hemagglutinin mutations that alter both antigenicity and
512		receptor binding avidity influence influenza virus antigenic clustering. J Virol 87:9904-
513		9910.
514	8.	Hensley SE, Das SR, Bailey AL, Schmidt LM, Hickman HD, Jayaraman A,
515		Viswanathan K, Raman R, Sasisekharan R, Bennink JR, Yewdell JW. 2009.
516		Hemagglutinin receptor binding avidity drives influenza A virus antigenic drift. Science
517		326: 734-736.
518	9.	Nelson MI, Vincent AL. 2015. Reverse zoonosis of influenza to swine: new perspectives
519		on the human-animal interface. Trends Microbiol 23:142-153.
520	10.	Belongia EA, Simpson MD, King JP, Sundaram ME, Kelley NS, Osterholm MT,
521		McLean HQ. 2016. Variable influenza vaccine effectiveness by subtype: a systematic

review and meta-analysis of test-negative design studies. Lancet Infect Dis 16:942-951.

523 11. Rajao DS, Perez DR. 2018. Universal Vaccines and Vaccine Platforms to Protect 524 against Influenza Viruses in Humans and Agriculture. Front Microbiol 9:123. 525 12. Altman MO, Bennink JR, Yewdell JW, Herrin BR. 2015. Lamprey VLRB response to 526 influenza virus supports universal rules of immunogenicity and antigenicity. Elife 4. 527 13. Virelizier JL. 1975. Host defenses against influenza virus: the role of anti-hemagglutinin 528 antibody. J Immunol 115:434-439. 529 14. Altman MO, Angeletti D, Yewdell JW. 2018. Antibody Immunodominance: The Key 530 to Understanding Influenza Virus Antigenic Drift. Viral Immunol 31:142-149. 531 Chambers BS, Parkhouse K, Ross TM, Alby K, Hensley SE. 2015. Identification of 15. 532 Hemagglutinin Residues Responsible for H3N2 Antigenic Drift during the 2014-2015 533 Influenza Season. Cell Rep 12:1-6. 534 16. Smith DJ, Lapedes AS, de Jong JC, Bestebroer TM, Rimmelzwaan GF, Osterhaus 535 **AD, Fouchier RA.** 2004. Mapping the antigenic and genetic evolution of influenza virus. 536 Science 305:371-376. 537 17. Koel BF, Burke DF, Bestebroer TM, van der Vliet S, Zondag GC, Vervaet G, 538 Skepner E, Lewis NS, Spronken MI, Russell CA, Eropkin MY, Hurt AC, Barr IG, 539 de Jong JC, Rimmelzwaan GF, Osterhaus AD, Fouchier RA, Smith DJ. 2013. 540 Substitutions near the receptor binding site determine major antigenic change during 541 influenza virus evolution. Science **342:**976-979. 542 Abente EJ, Santos J, Lewis NS, Gauger PC, Stratton J, Skepner E, Anderson TK, 18. 543 Rajao DS, Perez DR, Vincent AL. 2016. The Molecular Determinants of Antibody 544 Recognition and Antigenic Drift in the H3 Hemagglutinin of Swine Influenza A Virus. J

Virol 90:8266-8280.

546 19. Chen H, Ye J, Xu K, Angel M, Shao H, Ferrero A, Sutton T, Perez DR. 2012. Partial 547 and full PCR-based reverse genetics strategy for influenza viruses. PLoS One 7:e46378. 548 20. Perez DR, Angel M, Gonzalez-Reiche AS, Santos J, Obadan A, Martinez-Sobrido L. 549 2017. Plasmid-Based Reverse Genetics of Influenza A Virus. Methods Mol Biol 550 1602:251-273. Ito T, Suzuki Y, Mitnaul L, Vines A, Kida H, Kawaoka Y. 1997. Receptor specificity 551 21. 552 of influenza A viruses correlates with the agglutination of erythrocytes from different 553 animal species. Virology 227:493-499. 554 Medeiros R, Escriou N, Naffakh N, Manuguerra JC, van der Werf S. 2001. 22. 555 Hemagglutinin residues of recent human A(H3N2) influenza viruses that contribute to the 556 inability to agglutinate chicken erythrocytes. Virology 289:74-85. 557 23. Bradley KC, Galloway SE, Lasanajak Y, Song X, Heimburg-Molinaro J, Yu H, 558 Chen X, Talekar GR, Smith DF, Cummings RD, Steinhauer DA. 2011. Analysis of 559 influenza virus hemagglutinin receptor binding mutants with limited receptor recognition 560 properties and conditional replication characteristics. J Virol 85:12387-12398. 561 24. Matrosovich MN, Gambaryan AS. 2012. Solid-phase assays of receptor-binding 562 specificity. Methods Mol Biol 865:71-94. Peng W, de Vries RP, Grant OC, Thompson AJ, McBride R, Tsogtbaatar B, Lee PS, 563 25. 564 Razi N, Wilson IA, Woods RJ, Paulson JC. 2017. Recent H3N2 Viruses Have Evolved 565 Specificity for Extended, Branched Human-type Receptors, Conferring Potential for 566 Increased Avidity. Cell Host Microbe 21:23-34. Matrosovich MN, Gambaryan AS, Teneberg S, Piskarev VE, Yamnikova SS, Lvov 567 26.

DK, Robertson JS, Karlsson KA. 1997. Avian influenza A viruses differ from human

569		viruses by recognition of sialyloligosaccharides and gangliosides and by a higher
570		conservation of the HA receptor-binding site. Virology 233:224-234.
571	27.	Rogers GN, Paulson JC. 1983. Receptor determinants of human and animal influenza
572		virus isolates: differences in receptor specificity of the H3 hemagglutinin based on
573		species of origin. Virology 127: 361-373.
574	28.	Yamada S, Suzuki Y, Suzuki T, Le MQ, Nidom CA, Sakai-Tagawa Y, Muramoto Y,
575		Ito M, Kiso M, Horimoto T, Shinya K, Sawada T, Kiso M, Usui T, Murata T, Lin Y,
576		Hay A, Haire LF, Stevens DJ, Russell RJ, Gamblin SJ, Skehel JJ, Kawaoka Y. 2006.
577		Haemagglutinin mutations responsible for the binding of H5N1 influenza A viruses to
578		human-type receptors. Nature 444: 378-382.
579	29.	Gamblin SJ, Haire LF, Russell RJ, Stevens DJ, Xiao B, Ha Y, Vasisht N, Steinhauer
580		DA, Daniels RS, Elliot A, Wiley DC, Skehel JJ. 2004. The structure and receptor
581		binding properties of the 1918 influenza hemagglutinin. Science 303: 1838-1842.
582	30.	Rogers GN, Paulson JC, Daniels RS, Skehel JJ, Wilson IA, Wiley DC. 1983. Single
583		amino acid substitutions in influenza haemagglutinin change receptor binding specificity.
584		Nature 304: 76-78.
585	31.	Wu NC, Thompson AJ, Xie J, Lin CW, Nycholat CM, Zhu X, Lerner RA, Paulson
586		JC , Wilson IA . 2018. A complex epistatic network limits the mutational reversibility in
587		the influenza hemagglutinin receptor-binding site. Nat Commun 9: 1264.
588	32.	Lewis NS, Anderson TK, Kitikoon P, Skepner E, Burke DF, Vincent AL. 2014.
589		Substitutions near the hemagglutinin receptor-binding site determine the antigenic
590		evolution of influenza A H3N2 viruses in U.S. swine. J Virol 88:4752-4763.

591 33. Petrova VN, Russell CA. 2018. The evolution of seasonal influenza viruses. Nat Rev 592 Microbiol 16:47-60. 593 34. Barr IG, Russell C, Besselaar TG, Cox NJ, Daniels RS, Donis R, Engelhardt OG, 594 Grohmann G, Itamura S, Kelso A, McCauley J, Odagiri T, Schultz-Cherry S, Shu 595 Y, Smith D, Tashiro M, Wang D, Webby R, Xu X, Ye Z, Zhang W, Writing 596 Committee of the World Health Organization Consultation on Northern 597 Hemisphere Influenza Vaccine Composition f. 2014. WHO recommendations for the 598 viruses used in the 2013-2014 Northern Hemisphere influenza vaccine: Epidemiology, 599 antigenic and genetic characteristics of influenza A(H1N1)pdm09, A(H3N2) and B influenza viruses collected from October 2012 to January 2013. Vaccine 32:4713-4725. 600 601 35. Klimov AI, Garten R, Russell C, Barr IG, Besselaar TG, Daniels R, Engelhardt OG, 602 Grohmann G, Itamura S, Kelso A, McCauley J, Odagiri T, Smith D, Tashiro M, Xu 603 X, Webby R, Wang D, Ye Z, Yuelong S, Zhang W, Cox N, Writing Committee of the 604 World Health Organization Consultation on Southern Hemisphere Influenza 605 **Vaccine Composition f.** 2012. WHO recommendations for the viruses to be used in the 606 2012 Southern Hemisphere Influenza Vaccine: epidemiology, antigenic and genetic 607 characteristics of influenza A(H1N1)pdm09, A(H3N2) and B influenza viruses collected 608 from February to September 2011. Vaccine 30:6461-6471. 609 36. Govorkova EA, Matrosovich MN, Tuzikov AB, Bovin NV, Gerdil C, Fanget B, 610 Webster RG. 1999. Selection of receptor-binding variants of human influenza A and B 611 viruses in baby hamster kidney cells. Virology 262:31-38. Lin Y, Wharton SA, Whittaker L, Dai M, Ermetal B, Lo J, Pontoriero A, 612 37.

Baumeister E, Daniels RS, McCauley JW. 2017. The characteristics and antigenic

615		viruses passaged in MDCK cells. Influenza Other Respir Viruses 11:263-274.
616	38.	Tamura D, Nguyen HT, Sleeman K, Levine M, Mishin VP, Yang H, Guo Z, Okomo-
617		Adhiambo M, Xu X, Stevens J, Gubareva LV. 2013. Cell culture-selected substitutions
618		in influenza A(H3N2) neuraminidase affect drug susceptibility assessment. Antimicrob
619		Agents Chemother 57: 6141-6146.
620	39.	Mohr PG, Deng YM, McKimm-Breschkin JL. 2015. The neuraminidases of MDCK
621		grown human influenza A(H3N2) viruses isolated since 1994 can demonstrate receptor
622		binding. Virol J 12:67.
623	40.	Zost SJ, Parkhouse K, Gumina ME, Kim K, Diaz Perez S, Wilson PC, Treanor JJ,
624		Sant AJ, Cobey S, Hensley SE. 2017. Contemporary H3N2 influenza viruses have a
625		glycosylation site that alters binding of antibodies elicited by egg-adapted vaccine strains
626		Proc Natl Acad Sci U S A 114 :12578-12583.
627	41.	Aich U, Beckley N, Shriver Z, Raman R, Viswanathan K, Hobbie S, Sasisekharan R
628		2011. Glycomics-based analysis of chicken red blood cells provides insight into the
629		selectivity of the viral agglutination assay. FEBS J 278:1699-1712.
630	42.	Das SR, Hensley SE, David A, Schmidt L, Gibbs JS, Puigbo P, Ince WL, Bennink
631		JR, Yewdell JW. 2011. Fitness costs limit influenza A virus hemagglutinin glycosylation
632		as an immune evasion strategy. Proc Natl Acad Sci U S A 108:E1417-1422.
633	43.	Hensley SE, Das SR, Gibbs JS, Bailey AL, Schmidt LM, Bennink JR, Yewdell JW.
634		2011. Influenza A virus hemagglutinin antibody escape promotes neuraminidase
635		antigenic variation and drug resistance. PLoS One 6: e15190.

properties of recently emerged subclade 3C.3a and 3C.2a human influenza A(H3N2)

swine in Mexico. Elife 5.

636 44. Huang KY, Rijal P, Schimanski L, Powell TJ, Lin TY, McCauley JW, Daniels RS, 637 Townsend AR. 2015. Focused antibody response to influenza linked to antigenic drift. J 638 Clin Invest **125:**2631-2645. 639 Stark SE, Caton AJ. 1991. Antibodies that are specific for a single amino acid 45. 640 interchange in a protein epitope use structurally distinct variable regions. J Exp Med 641 **174:**613-624. Ekiert DC, Kashyap AK, Steel J, Rubrum A, Bhabha G, Khayat R, Lee JH, Dillon 642 46. 643 MA, O'Neil RE, Faynboym AM, Horowitz M, Horowitz L, Ward AB, Palese P, 644 Webby R, Lerner RA, Bhatt RR, Wilson IA. 2012. Cross-neutralization of influenza A 645 viruses mediated by a single antibody loop. Nature **489:**526-532. 646 47. Pena L, Vincent AL, Ye J, Ciacci-Zanella JR, Angel M, Lorusso A, Gauger PC, 647 Janke BH, Loving CL, Perez DR. 2011. Modifications in the polymerase genes of a 648 swine-like triple-reassortant influenza virus to generate live attenuated vaccines against 649 2009 pandemic H1N1 viruses. J Virol **85:**456-469. 650 48. Tang Y, Lee CW, Zhang Y, Senne DA, Dearth R, Byrum B, Perez DR, Suarez DL, 651 Saif YM. 2005. Isolation and characterization of H3N2 influenza A virus from turkeys. 652 Avian Dis 49:207-213. 653 49. Reed LJ, Muench H. 1938. A simple method for estimating fifty percent endpoints. Am 654 J Hyg 27:493-497. 655 Mena I, Nelson MI, Quezada-Monroy F, Dutta J, Cortes-Fernandez R, Lara-Puente 50. 656 JH, Castro-Peralta F, Cunha LF, Trovao NS, Lozano-Dubernard B, Rambaut A, 657 van Bakel H, Garcia-Sastre A. 2016. Origins of the 2009 H1N1 influenza pandemic in

660

661

51.

organization and analysis of sequence data. Bioinformatics 28:1647-1649. 662 663 52. Spackman E, Senne DA, Myers TJ, Bulaga LL, Garber LP, Perdue ML, Lohman K, 664 Daum LT, Suarez DL. 2002. Development of a real-time reverse transcriptase PCR 665 assay for type A influenza virus and the avian H5 and H7 hemagglutinin subtypes. J Clin 666 Microbiol 40:3256-3260. Santos JJS, Obadan AO, Garcia SC, Carnaccini S, Kapczynski DR, Pantin-667 53. Jackwood M, Suarez DL, Perez DR. 2017. Short- and long-term protective efficacy 668 669 against clade 2.3.4.4 H5N2 highly pathogenic avian influenza virus following prime-670 boost vaccination in turkeys. Vaccine 35:5637-5643. 54. 671 World Health Organization, 2011. Manual for the laboratory diagnosis and virological 672 surveillance of influenza. World Health Organization, Geneva. 673 55. Lakdawala SS, Lamirande EW, Suguitan AL, Jr., Wang W, Santos CP, Vogel L, 674 Matsuoka Y, Lindsley WG, Jin H, Subbarao K. 2011. Eurasian-origin gene segments 675 contribute to the transmissibility, aerosol release, and morphology of the 2009 pandemic 676 H1N1 influenza virus. PLoS Pathog 7:e1002443. 677 56. Stevens J, Chen LM, Carney PJ, Garten R, Foust A, Le J, Pokorny BA, 678 Manojkumar R, Silverman J, Devis R, Rhea K, Xu X, Bucher DJ, Paulson JC, Cox 679 NJ, Klimov A, Donis RO. 2010. Receptor specificity of influenza A H3N2 viruses 680 isolated in mammalian cells and embryonated chicken eggs. J Virol 84:8287-8299.

Kearse M, Moir R, Wilson A, Stones-Havas S, Cheung M, Sturrock S, Buxton S,

2012. Geneious Basic: an integrated and extendable desktop software platform for the

Cooper A, Markowitz S, Duran C, Thierer T, Ashton B, Meintjes P, Drummond A.

681 57. Eswar N, Webb B, Marti-Renom MA, Madhusudhan MS, Eramian D, Shen MY, 682 Pieper U, Sali A. 2006. Comparative protein structure modeling using Modeller. Curr 683 Protoc Bioinformatics Chapter 5:Unit-5 6. 684 58. Schrodinger, LLC. 2015. The PyMOL Molecular Graphics System, Version 2.1. 685 59. Zhang Y, Aevermann BD, Anderson TK, Burke DF, Dauphin G, Gu Z, He S, 686 Kumar S, Larsen CN, Lee AJ, Li X, Macken C, Mahaffey C, Pickett BE, Reardon B, Smith T, Stewart L, Suloway C, Sun G, Tong L, Vincent AL, Walters B, 687 688 Zaremba S, Zhao H, Zhou L, Zmasek C, Klem EB, Scheuermann RH. 2017. 689 Influenza Research Database: An integrated bioinformatics resource for influenza virus 690 research. Nucleic Acids Res 45:D466-D474.

Figure legends

692

693

694

695

696

697

698

699

700

701

702

703

704

705

706

707

708

709

710

711

712

713

714

Figure 1. Amino acid plasticity at residue 145. (A) Publicly available H3 HA sequences were retrieved and the relative frequency of identified amino acids at residue 145 were calculated for swine, human, avian, canine and equine AIVs. Amino acids present at frequency below 1% are not labeled in the figure. (B) Schematic representation of the HA gene segment of A/turkey/Ohio/313053/2004 (H3N2) depicting the codon corresponding to residue 145 and respective amino acid substitutions introduced by site-directed mutagenesis. (C) HA monomeric structure of A/turkey/Ohio/313053/2004 (H3N2) indicating the location of HA residue 145. Figure 2. Substitutions at residue 145 show no major impact on virus growth but decrease receptor binding avidity. A) Confluent monolayers of MDCK cells were inoculated with H3 viruses carrying amino acid substitutions at residue 145 at a MOI of 0.01 and incubated at 37°C. At 6, 12, 24, 48, and 72 hpi, tissue culture supernatants from inoculated cells were collected for virus RNA quantification by rRT-PCR and expressed as log₁₀ TCID₅₀/ml equivalents. Plotted data represent means ± standard errors (SD). Turkey red blood cells pretreated with different amounts of neuraminidase from either (B) Clostridium perfringens or (C) Arthrobacter ureafaciens were mixed with H3 viruses carrying amino acid substitutions at residue 145 to quantify virus agglutination as measure of virus binding avidity. Data are expressed as the maximal amount of neuraminidase that allowed full agglutination. (B) and (C) are representative data of one out of 2 and 3 independent experiments, respectively, with samples run in duplicates in each experiment. Plotted data represent means \pm standard errors (SD). Figure 3. Substitutions at residue 145 retain binding to SAα2-6Gal. H3 viruses carrying amino acid substitutions at residue 145 were tested for receptor binding specificity with varying

concentrations of $SA\alpha^2$ -3Gal (α^2 -3-linked SA) or $SA\alpha^2$ -6Gal (α^2 -6-linked SA). (A) 145N (wt),

715 (B) 145A, (C) 145F, (D) 145G, (E) 145H, (F) 145I, (G) 145K, (H) 145L, (I) 145M, (J) 145P, (K) 716 145Q, (L) 145R, (M) 145S, (N) 145T, (O) 145V and (P) 145Y viruses. (Q) Human pH1N1 and 717 (R) avian Δ H5N1 were used as binding control to SA α 2-6Gal and SA α 2-3Gal, respectively. 718 Glycan concentration is expressed as arbitrary units (AU). Plotted data represent means \pm 719 standard errors (SD). Data is representative of 2 independent experiments with 2 replicates per 720 experiment. 721 Figure 4. Substitutions at residue 145 modulate binding to a broad range of SAa2-6Gal 722 glycans. Glycan microarray analysis of H3 viruses carrying amino acid substitutions at residue 723 145. The array is comprised of non-sialoside control (1-10; Grey), SAα2-3Gal (11-76; Yellow) 724 and SAα2-6Gal (77-128; Green) glycans. Glycans are grouped by structure type: L, linear; O, O-725 linked; N, N-linked and L^x, sialyl Le^x. (A) 145N (wt), (B) 145A, (C) 145F, (D) 145G, (E) 145H, 726 (F) 145I, (G) 145K, (H) 145L, (I) 145M, (J) 145P, (K) 145Q, (L) 145R, (M) 145S, (N) 145T, (O) 727 145V and (P) 145Y viruses. Plotted data represent means ± standard errors (SD) using four 728 replicates per virus. RFU, relative fluorescent units. 729 Figure 5. Substitutions at residue 145 modulate sera reactivity. Antibody responses to H3 730 viruses carrying amino acid substitutions at residue 145 was determined by ELISA using swine 731 antisera generated against (A) OH/04, (B) NY/11 possessing HA residue 145N or (C) IA/14 732 possessing HA residue 145K. Two sets of sera were tested independently. The first set of sera 733 was tested 2 times in duplicates. The second set of sera was tested only once in duplicate. Plotted 734 data represent means \pm standard errors (SD). O.D., optical density. 735 Figure 6. Substitutions at residue 145 impact HI titers. HI titers were measured against H3 736 viruses carrying amino acid substitutions at residue 145 using swine antisera generated against

OH/04 (cyan), NY/11 possessing HA residue 145N (red) or IA/14 possessing HA residue 145K

739

740

741

742

743

(light green). (A and B) two sets of sera were tested independently. The first set of sera was tested 3 times in duplicates. Confirmatory tests were run on a second set of sera, which tested once in duplicates. Sera reactivity of all H3 mutant viruses to the respective swine antisera are depicted as fold change [(log2 HI titer mutant virus)/(log2 HI titer homologous virus)]. Plotted data represent means \pm standard errors (SD). Colors are based on the antigenic cluster designation for swine H3N2 IAVs.

Downloaded from http://jvi.asm.org/ on January 30, 2019 by guest

Tables 744

Table 1. Primers used to introduce amino acid substitutions at residue 145

aa at position 145	Forward primer sequence (5'-3')*	Reverse primer sequence (5'-3')*
A	${\tt GGAATCTGTT}{\tt GCT}{\tt AGTTTCTTTAGTAGATT}$	${\sf TAAAGAAACT} \textbf{AGC} {\sf AACAGATTCCCTTCT}$
C	$GGAATCTGTT\mathbf{TGT}AGTTTCTTTAGTAGATT$	TAAAGAAACT ACA AACAGATTCCCTTCT
D	$GGAATCTGTT \mathbf{GAT} AGTTTCTTTAGTAGATT$	TAAAGAAACT ATC AACAGATTCCCTTCT
E	$GGAATCTGTT \mathbf{GAA} AGTTTCTTTAGTAGATT$	TAAAGAAACT TTC AACAGATTCCCTTCT
F	GGAATCTGTT TT AGTTTCTTTAGTAGATT	TAAAGAAACT AAA AACAGATTCCCTTCT
G	$GGAATCTGTT \mathbf{GGA} AGTTTCTTTAGTAGATT$	TAAAGAAACT TCC AACAGATTCCCTTCT
Н	GGAATCTGTT CAT AGTTTCTTTAGTAGATT	TAAAGAAACT ATG AACAGATTCCCTTCT
I	GGAATCTGTT ATA AGTTTCTTTAGTAGATT	TAAAGAAACT TAT AACAGATTCCCTTCT
K	$GGAATCTGTT \boldsymbol{A} \boldsymbol{A} \boldsymbol{A} GGTTTCTTTAGTAGATT$	TAAAGAAACT TT AACAGATTCCCTTCT
L	GGAATCTGTT CTC AGTTTCTTTAGTAGATT	${\sf TAAAGAAACT} \textbf{GAG} {\sf AACAGATTCCCTTCT}$
M	$GGAATCTGTT \boldsymbol{ATG} AGTTTCTTTAGTAGATT$	TAAAGAAACT CAT AACAGATTCCCTTCT
P	$GGAATCTGTT\mathbf{CCA}AGTTTCTTTAGTAGATT$	${\sf TAAAGAAACT} \textbf{TGG} {\sf AACAGATTCCCTTCT}$
Q	$GGAATCTGTT \boldsymbol{CAA} AGTTTCTTTAGTAGATT$	TAAAGAAACT TTG AACAGATTCCCTTCT
R	$GGAATCTGTT \boldsymbol{CGG} \boldsymbol{AGTTTCTTTAGTAGATT}$	TAAAGAAACTCCGAACAGATTCCCTTCT
S	$GGAATCTGTT \boldsymbol{\mathbf{AGC}} AGTTTCTTTAGTAGATT$	TAAAGAAACT GCT AACAGATTCCCTTCT
T	$GGAATCTGTT \boldsymbol{ACA} AGTTTCTTTAGTAGATT$	TAAAGAAACT TGT AACAGATTCCCTTCT
V	${\tt GGAATCTGTT} {\tt GTC} {\tt AGTTTCTTTAGTAGATT}$	${\sf TAAAGAAACT} \textbf{GAC} {\sf AACAGATTCCCTTCT}$
W	$GGAATCTGTT \mathbf{T} \mathbf{G} GAGTTTCTTTAGTAGATT$	TAAAGAAACT CCA AACAGATTCCCTTCT
Y	GGAATCTGTT TAT AGTTTCTTTAGTAGATT	TAAAGAAACT ATA AACAGATTCCCTTCT

^{*}Bold nucleotides indicate the mutated codon associated to HA residue 145.

745

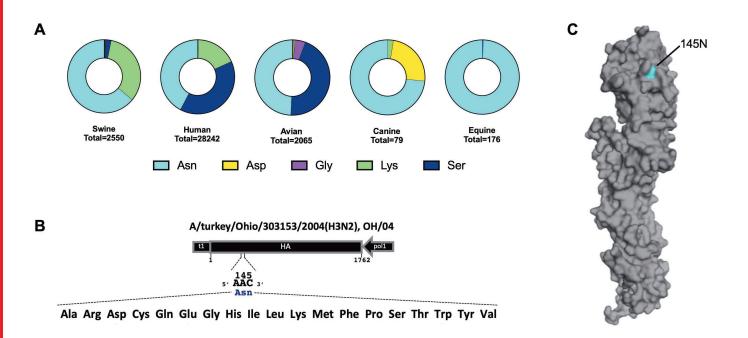
746

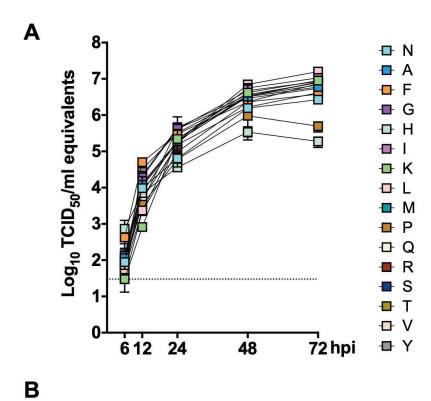
Downloaded from http://jvi.asm.org/ on January 30, 2019 by guest

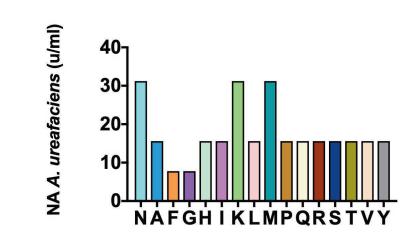
Table 2. Agglutination of erythrocytes by OH/04 145 single aa mutant viruses

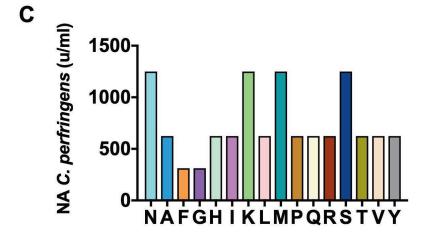
aa at position 145	HA titer (HAU)		
	0.5% turkey RBCs	0.5% chicken RBCs	1% horse RBCs
N (wt)	128	256	<2
A	128	64	<2
C	4	<2	<2
F	128	16	8
G	128	32	<2
Н	256	128	<2
I	128	64	<2
K	128	128	<2
L	128	128	<2
M	128	128	<2
P	128	64	<2
Q	256	128	<2
R	128	64	<2
S	128	128	<2
T	128	64	<2
V	128	32	<2
Y	128	32	<2

Downloaded from http://jvi.asm.org/ on January 30, 2019 by guest









 \leq

